

**Identification, classification, and signal amplification capabilities
of high-turnover gas binding hosts in ultra-sensitive NMR**

– **Electronic Supporting Information** –

Martin Kunth,^{*} Christopher Witte, and Leif Schröder[†]
*ERC Project BiosensorImaging, Leibniz-Institut für
Molekulare Pharmakologie (FMP), 13125 Berlin, Germany*

Andreas Hennig
*Jacobs University Bremen, Department of Life Sciences and Chemistry,
Campus Ring 1, 28759 Bremen, Germany*

CONTENTS

S1: CB6 Modeling	S3
S2: Xe-CrA Exchange Kinetics in Water	S4
S3: CB6-Line Broadening	S5
S4: Xe-CrA Exchange Kinetics in DMSO	S6
S5: Xe-Host Properties for Efficient Hyper-CEST Detection	S7
S6: Commercially Available Cucurbit[6]uril Sample by Sigma-Aldrich	S9
S7: Xe Delivery Into H ₂ O and DMSO	S10
References	S11

S1: CB6 MODELING

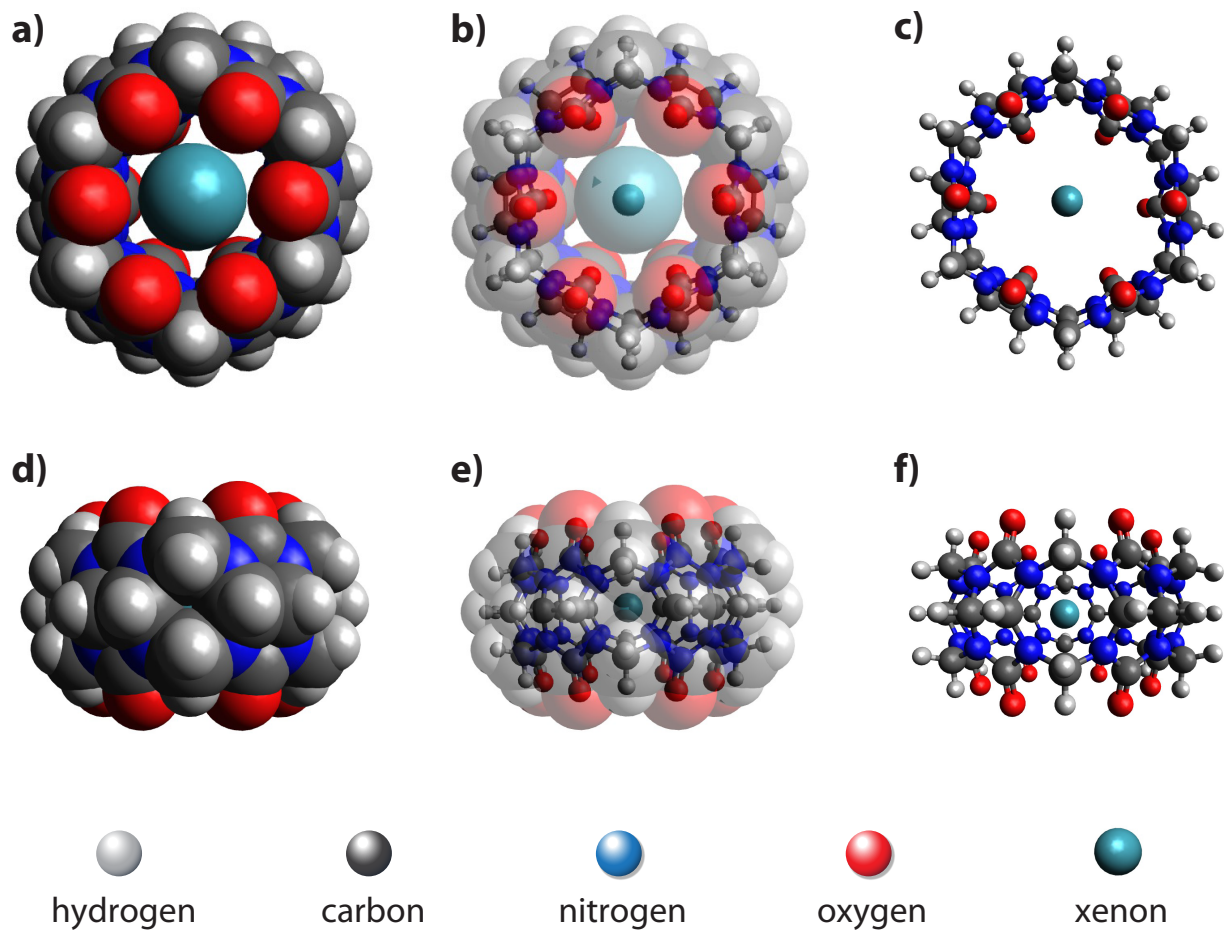


FIG. S1. Cucurbit[6]uril (CB6) ($C_{36}H_{36}N_{24}O_{12}$) and xenon (Xe) modeling using the open-source molecular builder and visualization tool, Avogadro – Version 1.1.1[1] (<http://avogadro.openmolecules.net>). a) Xe encapsulation by CB6 in the van der Waals radius representation from the top view of the molecule. b) transparent overlay of the van der Waals radius representation shown in a) with the ball-and-stick model that is solely shown in c). d-f) displays the side view representation of a-c), respectively.

S2: XE-CRA EXCHANGE KINETICS IN WATER

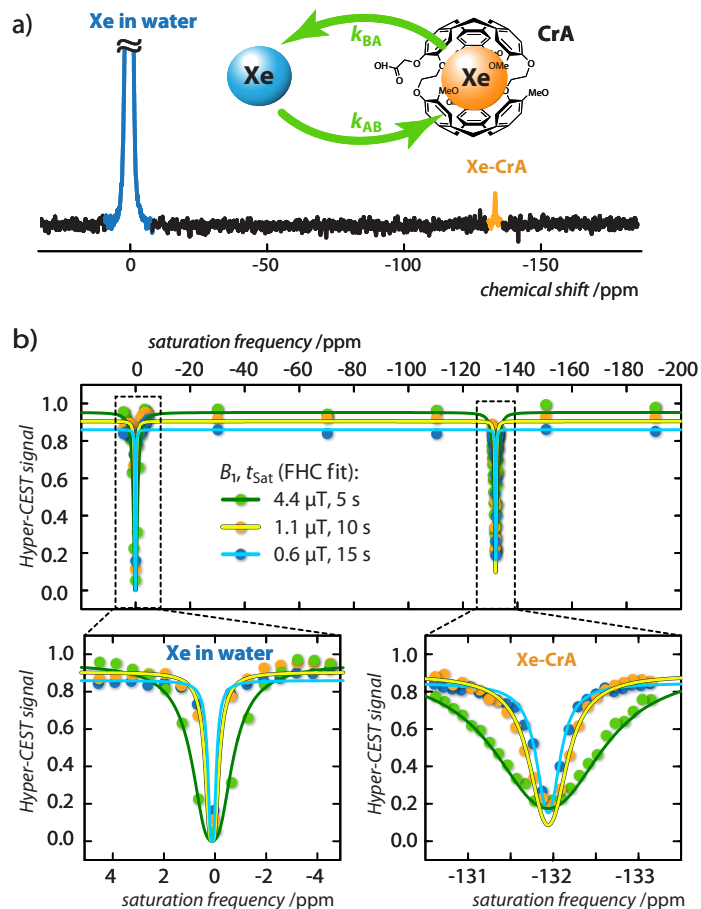


FIG. S2. Direct and indirect Hyper-CEST ^{129}Xe NMR measurements for $[\text{CrA}] = 11 \mu\text{M}$ dissolved in pure water at room temperature, $T = 295 \text{ K}$. a) ^{129}Xe NMR spectrum with 64 averages. The Xe-CrA resonance appears at $\delta_{\text{B}} = -132 \text{ ppm}$. b) Hyper-CEST z -spectra (dots) for continuous-wave (cw) saturation of $B_1/t_{\text{sat}} = \{4.4/5 \text{ (green)}, 1.1/10 \text{ (orange)}, 0.6/15 \text{ (blue)}\} \mu\text{T/s}$ including global fitting curves of the full Hyper-CEST (FHC) solution (solid lines). The fitting results are listed in Table 1 in the main manuscript.

S3: CB6-LINE BROADENING

In chemical equilibrium the following equation holds

$$[\text{Xe}] \underbrace{[\text{CB6}] k_{\text{AB}}}_{k'} = [\text{Xe@CB6}] k_{\text{BA}} .$$

We therefore have

$$k' = \frac{[\text{Xe@CB6}]}{[\text{Xe}]} k_{\text{BA}} = f_{\text{B}} k_{\text{BA}} .$$

The linewidth (full width at half maximum, FWHM) for each spin pool is influenced by the transverse relaxation and the exchange rate out of the particular spin pool according to the following equation (M.T. McMAHON *et al.*[2] and citations therein),

$$\text{FWHM} = (k + R_2)/\pi .$$

The FWHM of the solution pool yields

$$\begin{aligned} \text{FWHM}_{\text{sol}} &= (k' + R_{2,\text{sol}})/\pi \\ &= (f_{\text{B}} \cdot k_{\text{BA}} + R_{2,\text{sol}})/\pi \end{aligned}$$

Thus, the exchange broadening contribution is

$$\begin{aligned} \Delta\nu_{\text{sol,ex}} &= (0.0043 \cdot 2,100 \text{ s}^{-1})/\pi \\ &\sim 3 \text{ Hz} , \end{aligned}$$

using the numbers listed in Table 1 in the main manuscript. We measured the FWHM_{sol} (of Figure 2a in the main manuscript) to be 22 Hz (at 9.4 T) for a 10 mm NMR tube; ca. 1.5 mL solution. Thus, we can see that the contribution of exchange broadening to the solution pool linewidth is not significant.

In contrast, the line broadening of the CB6-bound Xe resonance is significant:

$$\begin{aligned} \text{FWHM}_{\text{CB6}} &= (k_{\text{BA}} + R_{2,\text{CB6}})/\pi \\ \Rightarrow \Delta\nu_{\text{CB6,ex}} &= (2,100 \text{ s}^{-1})/\pi \\ &\sim 670 \text{ Hz} . \end{aligned}$$

Intuitively, the majority of the pool of Xe@CB6 is participating in exchange at any time, leading to a large linewidth, but the residence time in the much larger solution pool is significantly longer, thus leading to a narrow resonance.

S4: XE-CRA EXCHANGE KINETICS IN DMSO

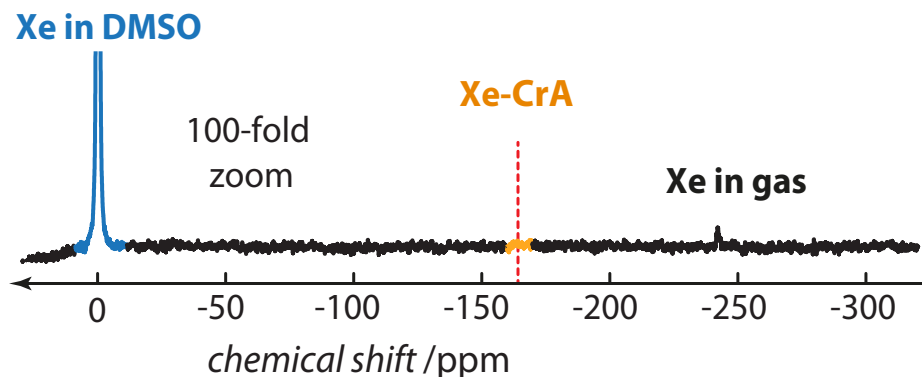


FIG. S4. Direct ^{129}Xe NMR spectrum with 100-fold zoom as average of 16 scans of $50\ \mu\text{M}$ of CrA in dimethyl sulfoxide (DMSO) at $T = 295\ \text{K}$. The red dashed line indicates the chemical shift of the Xe-CrA in DMSO resonance. The results of a qHyper-CEST analysis of this sample are listed in Table I which agree well with previously reported results[3].

TABLE I. qHyper-CEST results for CrA in DMSO (at $T = 295\ \text{K}$). The listed parameters are identical with those of Table 1 in the main manuscript.

solvent	$[\text{Xe}]^a$	host	$[\text{host}_{\text{tot}}]$	$\Delta\delta$ (ppm)	f_{B} (10^{-4})	k_{BA} (s^{-1})	β (%) ^b	K_{A} (M^{-1}) ^c	$[\text{host}_{\text{occ}}]$	$\beta \cdot k_{\text{BA}}$
	(μM)		(μM)						(μM)	(% s^{-1})
DMSO	2,340	CrA	50	-166.37 ± 0.04	18 ± 1	250 ± 130	9	38 ± 4	4.5	23

^a Calculation given in the Experimental Section. ^b As given by Eq. 3 in Ref. 3. ^c As given by Eq.

4 in Ref. 3.

S5: XE-HOST PROPERTIES FOR EFFICIENT HYPER-CEST DETECTION

We derive the depolarization rate per host molecule from the ^{129}Xe depolarization rate, λ_{depol} , for on-resonant saturation (in the limit of $k_{\text{BA}} \gg R_2^{\text{B}}$), as reported in Ref.[3], divided by total host concentration, $[\text{host}]$, and multiplied by Xe concentration free in solution, $[\text{Xe}]$, to

$$\lambda_{\text{depol}}(B_1, k_{\text{BA}}) = f_{\text{B}} k_{\text{BA}} \frac{(\gamma B_1)^2}{(\gamma B_1)^2 + k_{\text{BA}}^2} \quad (1)$$

$$\Leftrightarrow \lambda_{\text{depol}}(B_1, k_{\text{BA}}) \cdot \frac{[\text{Xe}]}{[\text{host}]} = \beta \cdot k_{\text{BA}} \underbrace{\frac{(\gamma B_1)^2}{(\gamma B_1)^2 + k_{\text{BA}}^2}}_{= \alpha}, \quad (2)$$

with saturation pulse strength, B_1 , the exchange rate, k_{BA} , the ratio of bound and free Xe, f_{B} , the gyromagnetic ratio, γ , and the host occupancy, β . We used the identity $f_{\text{B}} = \beta \cdot \frac{[\text{host}]}{[\text{Xe}]}$ for rewriting Eq.(1) to obtain the gas turnover rate, $\beta \cdot k_{\text{BA}}$. Figure S5a shows the dependence of Eq.(2) with respect to the saturation pulse power, B_1 , for the Xe-host systems: CB6 in water (green), CrA in water (blue) and CrA in DMSO (red) using the values reported in Table 1 of the main manuscript. Figures S5b-c show its dependence versus the exchange rate, k_{BA} . Note that the maxima of these curves occur for the saturation pulse strength calculated in Hz.

In terms of Xe-host design for Hyper-CEST detection, Eq.(2) can be very useful because it shows that CB6 in water is indeed the superior system due to both relatively high occupancy and high exchange rate compared to CrA in water and in DMSO.

It also shows that at low saturation strength the Hyper-CEST performance is better for lower exchange rates (compare in the insert of Figure S5a; CrA in water and CB6 in water (blue and green, respectively)), since the Hyper-CEST labeling efficiency, α , in the limit of $k_{\text{BA}} \gg R_2^{\text{B}}$ is increased for decreased exchange rates, k_{BA} [4, 5].

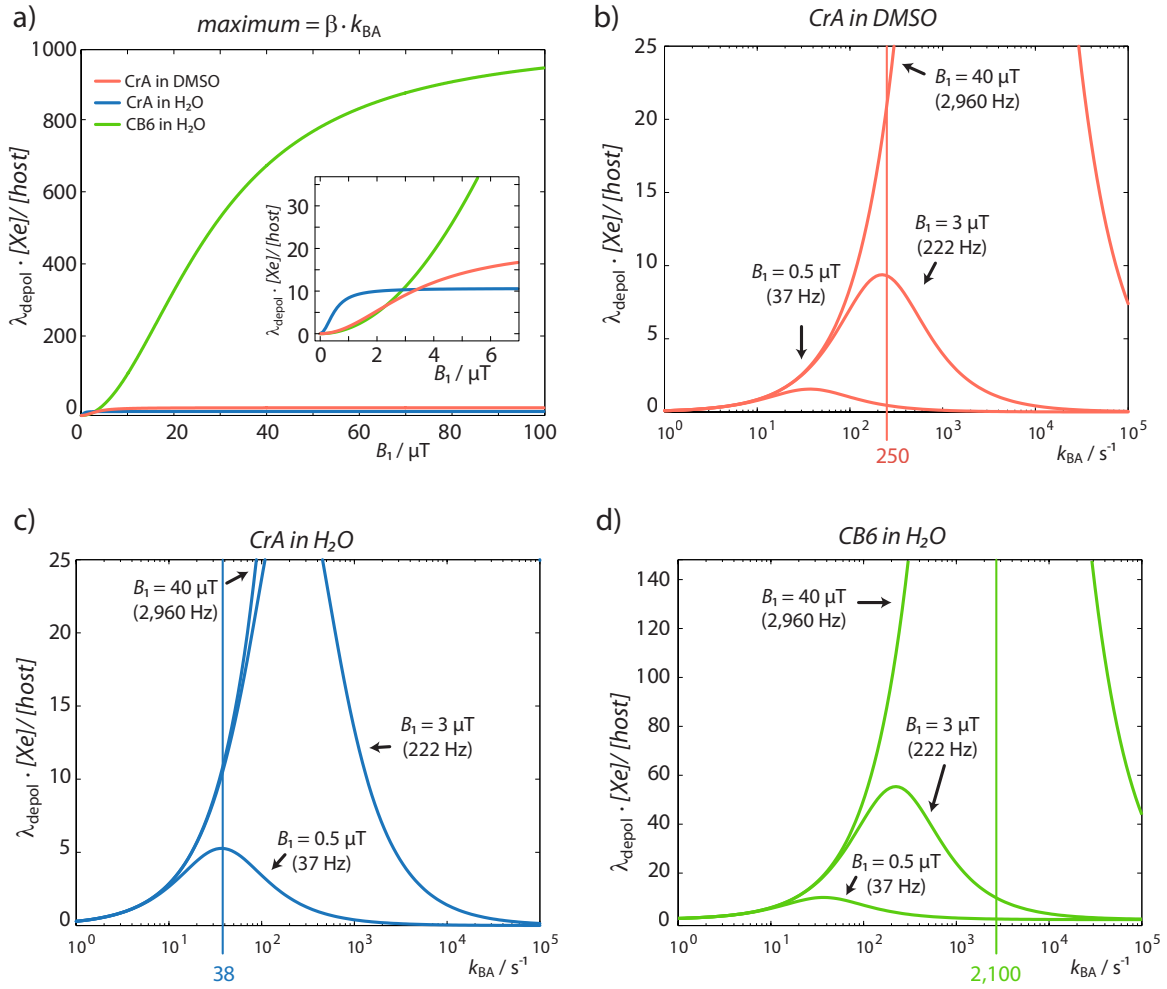


FIG. S5. Maximal on-resonant ^{129}Xe depolarization per host concentration in given Xe concentration for the Xe-host systems: CrA in DMSO (red), CrA in H_2O (blue) and CB6 in H_2O (green). The simulation parameters are listed in Table 1 in the main manuscript. (a) Xe depolarization curve per host molecule as a function of the saturation pulse strength, B_1 . (b-d) Xe depolarization curve divided by $[\text{host}]$ versus the exchange rate, k_{BA} , for the individual Xe-host systems with three different saturation pulse strengths, $B_1 = \{0.5, 3, 40\} \mu\text{T} \rightarrow \omega_1 = \gamma \cdot B_1 = \{37, 22, 2960\}$ Hz, respectively. The system intrinsic Xe exchange rates are indicated by the straight line.

S6: COMMERCIALY AVAILABLE CUCURBIT[6]URIL SAMPLE BY SIGMA-ALDRICH

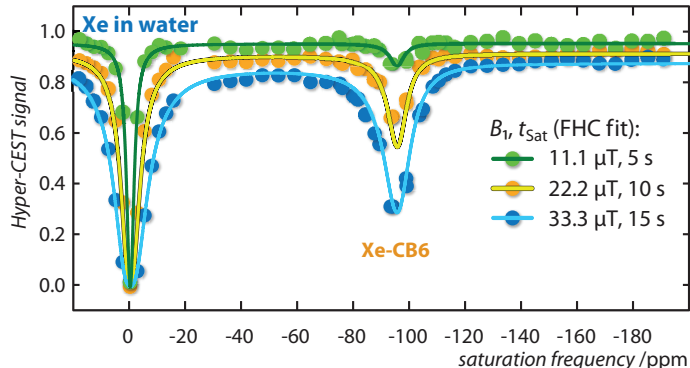


FIG. S6. qHyper-CEST analysis and results listed in Table II of the commercially available cucurbit[6]uril (CB6) sample (ordered by Sigma-Aldrich, product number: 94544, CAS Number: 80262-44-8, LOT Number: BCBH8803V) in water at room temperature ($T = 295$ K). In contrast to Figure 2b in the main manuscript, note that the saturation pulse strength values, B_1 , are increased and the Hyper-CEST z -spectra spectrally broadened.

While the relative chemical shift between free and bound Xe, $\Delta\delta$, and the Xe exchange rate, k_{BA} , agree with the pure CB6 sample (see main manuscript), the ratio of bound and free Xe, f_B , the Xe host occupancy, β , the Xe binding (association) constant, K_A , the host concentration occupied by Xe, $[\text{host}_{\text{occ}}] = \beta \cdot [\text{host}]$, and the gas turnover $\beta \cdot k_{BA}$ disagree (see Table II). This particular change of the specific Xe exchange kinetics indicates a blocking of Xe exchange for the CB6 portals for the commercially available sample.

TABLE II. qHyper-CEST results for the Sigma-Aldrich available CB6 sample in water (at $T = 295$ K). The listed parameters are identical with those of Table 1 in the main manuscript except for the host occupancy, β , the binding constant, K_A and its continuative values.

solvent	[Xe] ^a	host	[host _{tot}]	$\Delta\delta$ (ppm)	f_B (10^{-4})	k_{BA} (s^{-1})	β (%) ^b	K_A (M^{-1}) ^c	[host _{occ}]	$\beta \cdot k_{BA}$
	(μM)		(μM)						(nM)	(% s^{-1})
water	390	CB6	4.6	(-95.6 ± 0.2)	(0.7 ± 0.07)	$(2,100 \pm 500)$	0.6	(15 ± 7)	28	13

^a Calculation given in the Experimental Section in the main manuscript;

^b As given by Eq. 3 in Ref.[3]; ^c As given by Eq. 4 in Ref.[3].

S7: XE DELIVERY INTO H₂O AND DMSO

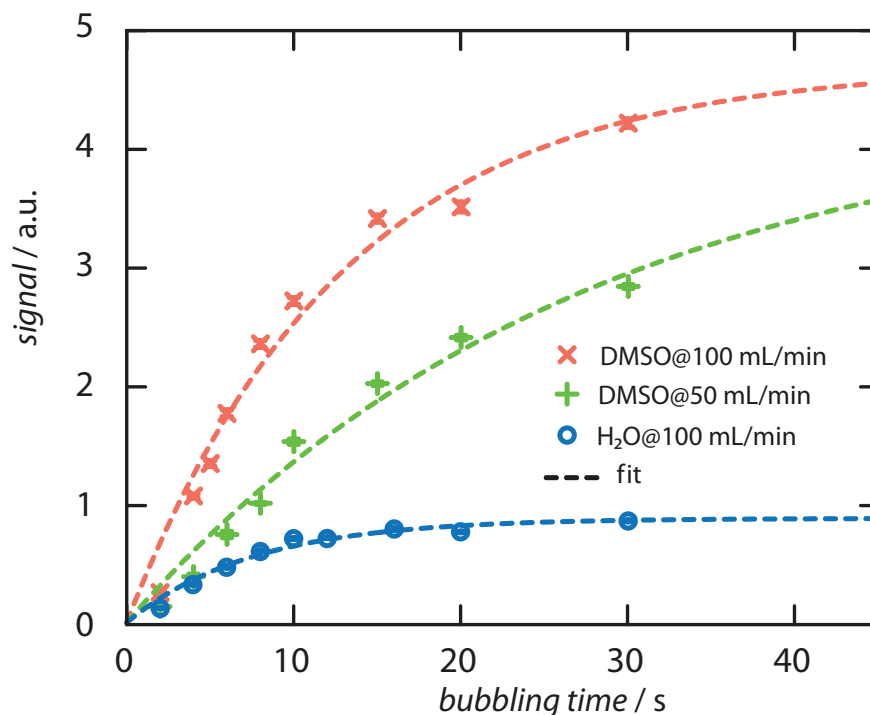


FIG. S7. Xe signal build up in H₂O and DMSO versus the bubbling time for flow rates of 50 mL per minute and 100 mL per minute including error bars.

Fit function with respect to the bubbling time, BT : $S(BT) = A_0 \cdot (1 - \exp\{-BT/\tau\})$. The total measured signal is influenced by the build up due to hp Xe bubbling while hp Xe starts to decay with its longitudinal relaxation time, T_1^A (~ 125 s for both solvents). Therefore, the ratio of $A_{0,\text{DMSO}}/A_{0,\text{H}_2\text{O}} \sim 5$ and differs from the value 6, as expected from the ratio of both Ostwald solubility coefficients.

- H₂O at 100 mL per minute: $A_0 = (0.88 \pm 0.04)$, $\tau = (8 \pm 1)$ s.
- DMSO at 100 mL per minute: $A_0 = (4.7 \pm 0.4)$, $\tau = (13 \pm 2)$ s.
- DMSO at 50 mL per minute: $A_0 = (4.4 \pm 0.9)$, $\tau = (27 \pm 8)$ s.

* kunth@fmp-berlin.de

† lschroeder@fmp-berlin.de

- [1] Hanwell, Marcus D.; Curtis, Donald E.; Lonie, David C.; Vandermeersch, Tim; Zurek, Eva; Hutchison, Geoffrey R. *Journal of Cheminformatics* **2012**, *4*, 17, <http://www.jcheminf.com/content/4/1/17>, <http://avogadro.openmolecules.net>.
- [2] McMahon, M.T.; Gilad, A.A.; Zhou, J.; Sun, P.Z.; Bulte, J.W.M.; van Zijl, P.C.M. *Magnetic Resonance in Medicine* **2006**, *55*, 863, <http://dx.doi.org/10.1002/mrm.20818>.
- [3] Kunth, M.; Witte, C.; Schröder, L. *The Journal of Chemical Physics* **2014**, *141*, 194202, <http://dx.doi.org/10.1063/1.4901429>.
- [4] Sun, P.Z.; Farrar, C.T.; Sorensen, A.G. *Magnetic Resonance in Medicine* **2007**, *58*, 1207-1215, <http://dx.doi.org/10.1002/cmml.1524>.
- [5] Zaiss, M.; Bachert, P. *NMR in Biomedicine* **2012**, *26*, 507-518, <http://dx.doi.org/10.1002/nbm.2887>.